High expression of trimethylated histone H3 at lysine 27 predicts better prognosis in non-small cell lung cancer

XIAOHUI CHEN[1,4], NING SONG[1], KEITARO MATSUMOTO[2], ATSUSHI NANASHIMA[2], TAKESHI NAGAYASU[2], TOMAYOSHI HAYASHI[3], MINGANG YING[4], DAISUKE ENDO[1], ZHIREN WU[1] and TAKEHIKO KOJI[1]

[1]Department of Histology and Cell Biology; [2]Division of Surgical Oncology, Department of Translational Medical Sciences, Nagasaki University Graduate School of Biomedical Science; [3]Department of Pathology, Nagasaki University Hospital, Nagasaki, Japan; [4]Division of Oncological Surgery, Fujian Provincial Cancer Hospital, Teaching Hospital of Fujian Medical University, Fujian, P.R. China

Received April 14, 2013; Accepted June 3, 2013

DOI: 10.3892/ijo.2013.2062

Abstract. Epigenetic parameters such as DNA methylation and histone modifications play pivotal roles in carcinogenesis. Global histone modification patterns have been implicated as possible predictors of cancer recurrence and prognoses in a great variety of tumor entities. Our study was designed to evaluate the association among trimethylated histone H3 at lysine 27 (H3K27me3), clinicopathological variables and outcome in early-stage non-small cell lung cancer (NSCLC). The expression of H3K27me3 and its methyltransferase, enhancer of zeste homolog 2 (EZH2) together with proliferating cell nuclear antigen (PCNA) were evaluated by immunohistochemistry in normal lung tissue (n=5) and resected NSCLC patients (n=42). In addition, the specificity of antibody for H3K27me3 was tested by western blot analysis. The optimal cut-off point of H3K27me3 expression for prognosis was determined by the X-tile program. The prognostic significance was determined by means of Kaplan-Meier survival estimates and log-rank tests. As a result, enhanced trimethylation of H3K27me3 was correlated with longer overall survival (OS) and better prognosis (P<0.05). Moreover, both univariate and multivariate analyses indicated that H3K27me3 level was a significant and independent predictor of better survival (hazard ratio, 0.187; 95% confidence interval, 0.066-0.531, P=0.002). Furthermore, H3K27me3 expression was positively correlated with DNA methylation level at CCGG sites while reversely related to EZH2 expression (P<0.05). In conclusion, H3K27me3 level defines unrecognized subgroups of NSCLC patients with distinct epigenetic phenotype and clinical outcome, and can probably be used as a novel predictor for better prognosis in NSCLC patients.

Correspondence to: Professor Takehiko Koji, Department of Histology and Cell Biology, Nagasaki University Graduate School of Biomedical Sciences, 1-12-4 Sakamoto, Nagasaki 852-8523, Japan
E-mail: tkoji@nagasaki-u.ac.jp

Abbreviations: NSCLC, non-small cell lung cancer; H3K27me3, trimethylated histone H3 at lysine 27; EZH2, enhancer of zeste homolog 2; PCNA, proliferating cell nuclear antigen; OS, overall survival; DNMTs, DNA methyltransferase; SUZ12, suppressor of zeste 12; EED, embryonic ectoderm development; RBBP, retinoblastoma binding protein; PRC2, polycomb repressive complex 2; HELMET, histo endonuclease-linked detection of methylation sites of DNA

Key words: non-small cell lung cancer, trimethylated histone H3 at lysine 27, epigenetics, enhancer of zeste homolog 2, DNA methylation

Introduction

Lung cancer is still the leading cause of cancer death in both sexes throughout the world. More people die of lung cancer than of colon, breast, and prostate cancers combined, i.e., more than 1.2 million deaths each year (1). Non-small cell lung cancer (NSCLC) accounts for approximately 85-90% of all lung cancers. The poor prognosis of NSCLC is mainly due to late diagnosis, in as much as only 20 to 30% of patients are eligible for surgical resection. Despite the development of new chemotherapeutic drugs and multimodal treatment strategies, the survival rate of NSCLC remains unchanged and poor. Identification of new prognostic markers for the characterization of lung-cancer biology may be helpful, as they could serve as a basis for predicting response to radiation and chemotherapy at a molecular level.

The alterations in epigenomes such as DNA methylation and histone modifications play pivotal roles in carcinogenesis (2-4). It has been reported that DNA methylation level and global histone modification patterns may be possible predictors of cancer recurrence and prognosis in a large variety of cancer entities (5,6). Post-translational modification of histone tails alters the physical state of chromatin and has an essential role in both transcriptional repression and activation during embryonic development, lineage specification, terminal differ-

entiation and tumorigenesis as well (7,8). One such repressive modification, the trimethylation of lysine 27 on histone H3 (H3K27me3), seemed to be an epigenetic label mediating gene silencing; and a mark for *de novo* DNA methylation in cancer cells by recruitment of DNA methyltransferase (DNMTs) (9-11), contributing to tumor progression through suppression of a certain gene expression (12). In fact, many recent studies have revealed that H3K27me3 may be involved in the characterization of various types of human cancers, including breast cancer (5,13), hepatocellular carcinoma (14), prostate cancer (15), Hodgekin's lymphoma (16), esophageal cancer (17) and nasopharyngeal carcinoma (18). Reports of H3K27me3 levels in different cancer samples are somewhat contradictory. It is demonstrated that low H3K27me3 levels predicted poor outcome in breast, ovarian and pancreatic cancers (5) while high levels predicted poor outcome in hepatocellular carcinoma (14) and esophageal squamous cell carcinoma (17).

Moreover, H3K27 methylation is catalyzed by the SET domain of its specific methyltransferase, enhancer of zeste homolog 2 (EZH2), and requires the presence of 2 additional proteins, i.e., suppressor of zeste 12 (SUZ12) and embryonic ectoderm development (EED) (19). These proteins, together with the histone binding proteins retinoblastoma binding protein 4 (RBBP4) and RBBP7, comprise the core components of the polycomb repressive complex 2 (PRC2). Overexpression of EZH2 was also found in a variety of cancers, including lung cancer (20,21), breast cancer (5,22-26), melanoma (27), colorectal (20) and pancreatic adenocarcinoma (28) and ovarian carcinoma (29), and turned out to be closely associated with high proliferation rate and aggressive tumor subgroups, resulting in worse clinical outcome thereafter. Although many reports on the role of H3K27me3 in carcinogenesis are available, its carcinogenic role in NSCLC and how it interacts with EZH2 and DNA methylation remain unclear.

In the present study, we investigated the prognostic value of immunostaining for H3K27me3 and its relationship with EZH2 expression in NSCLC patients. We examined the correlation between these parameters and the level of DNA methylation at CCGG sites, detected by histo-endonuclease-linked detection of methylation sites of DNA (HELMET) (30). Since there had been several reports to indicate that H3K27me3 and EZH2 were involved in the early stage of various cancers, we focused on stage I NSCLCs in this study.

Materials and methods

Patients and tissue preparation. Five normal lung tissue and 42 NSCLC patients (22 adenocarcinomas and 20 squamous cell carcinomas) with early-stage (stage I) were included in our study. Patients underwent radical resection of primary tumor (lobectomy or pneumonectomy) and systematic lymphadenectomy at the First Department of Surgery, Nagasaki University Hospital (Nagasaki, Japan), between 2000 and 2006. The patients' clinicopathological data are shown in Table I. None of the patients had received chemo- or radiotherapy before tissue collection. The histopathologic features of the tumor specimens were classified in accordance with the WHO criteria. The TNM staging was determined according to the latest National Comprehensive Cancer Network (NCCN, Version 2, 2013) guidelines for NSCLC. The study protocol was approved by the Human Ethics Review Committee of Nagasaki University School of Medicine, and a signed informed consent was obtained from each patient. Each specimen was fixed overnight in 10% buffered formalin at room temperature (RT) and embedded in paraffin. Serial sections were cut at a thickness of 4 μm and placed onto 3-aminopropyltriethoxysilane-coated glass slides. Some sections were stained with hematoxylin and eosin in a routine manner for histological examination.

Chemicals and biochemicals. Bovine serum albumin (BSA) (essentially fatty acid and globulin-free), Trizma base, 2-mercaptoethanol, 3-aminopropyltriethoxysilane, Triton X-100, and Brij-35 were from Sigma Chemical Co. (St. Louis, MO, USA). Sodium dodecyl sulfate (SDS)-polyacrylamide gel electrophoresis (PAGE) reagents and the molecular marker set were purchased from Daiichi Pure Chemicals (Tokyo, Japan). Polyvinylidene fluoride membrane (PVDF) was purchased from Millipore (MA, USA). Lima bean trypsin inhibitor was purchased from Worthington Biochemical (Lakewood, NJ, USA); the protein assay kit and Coomassie Brilliant Blue were purchased from Bio-Rad Laboratories (Hercules, CA, USA); and 3,3'-diaminobenzidine-4HCl (DAB) was purchased from Dojin Chemical Co. (Kumamoto, Japan). Biotin-16-dUTP, digoxigenin-11-dUTP, Rhodamine anti-Dig and terminal deoxynucleotidyl transferase (TdT) were from Roche Diagnostics (Mannheim, Germany). Dideoxy ATP (ddATP) and dideoxy TTP (ddTTP) were from Jena Bioscience (Jena, Germany). *Hpa*II and *Msp*I were from Takara Bio Inc. (Shiga, Japan). 4',6-diamidino-2-phenyl-indole, dihydrochloride (DAPI) was from Invitrogen Corporation (Carlsbad, CA, USA). Permount was from Fisher Scientific Inc. (Bridgewater, NJ, USA). All other reagents used in this study were from Wako Pure Chemicals (Osaka, Japan) and were of analytical grade.

Immunohistochemistry for H3K27me3, EZH2, PCNA and simultaneous localization of EZH2 and PCNA. Immunohistochemistry was performed with the indirect enzyme-labeled antibody method, as described previously (31-33). Antibodies used in IHC are listed in Table II. For detection of H3K27me3, EZH2 and PCNA, paraffin-embedded sections were deparaffinized with toluene and rehydrated in graded alcohols. After autoclaved for 15 min at 120˚C in 10 mM citrate buffer (pH 6.0) for antigen retrieval, endogenous peroxidase was inactivated with 0.3% hydrogen peroxide in methanol for 15 min. The sections were then pre-incubated with 500 μg/ml normal goat IgG dissolved in 1% BSA in PBS (pH 7.4) for 1 h, reacted with primary antibodies for 16 h, washed with 0.075% Brij 35 in PBS, and then incubated with HRP-conjugated goat anti-rabbit IgG (H3K27me3/EZH2) or HRP-conjugated goat anti-mouse IgG (PCNA) in 1% BSA in PBS for 1 h. After washing with 0.075% Brij 35 in PBS, the sites of HRP were visualized with DAB and H_2O_2 in the presence of nickel and cobalt ions (34). As a negative control, some sections were reacted with normal rabbit IgG or normal mouse IgG instead of the specific antibodies. For simultaneous staining of EZH2 and PCNA, the sections were

Table I. Clinicopathologic parameters.

Parameters	No. of cases (%)	
	Adeno-carcinoma	Squamous cell carcinoma
Median age, years	68.50	69.75
Age (y.o.)		
≤69	12 (54.5)	12 (60)
>69	10 (45.5)	8 (40)
Gender		
Male	10 (45.5)	17 (85)
Female	12 (54.5)	3 (15)
Serum CEA (ng/ml)		
≤5	22 (100)	17 (85)
>5	0	3 (15)
P-factor		
Positive	1 (4.5)	0
Negative	21 (95.5)	20 (100)
LV-factor		
Positive	18 (81.8)	13 (65)
Negative	4 (18.2)	7 (35)
V-factor		
Positive	8 (36.4)	10 (50)
Negative	14 (63.6)	10 (50)
T-stage		
1a	16 (72.7)	13 (65)
1b	5 (22.7)	7 (35)
2a	1 (4.6)	
Nodal status		
N0	22 (100)	20 (100)
Differentiation		
Well	13 (59.1)	3 (15)
Moderate	6 (27.3)	9 (45)
Poor	3 (13.6)	8 (40)
Relapse		
Yes	2 (9.1)	8 (40)
No	20 (90.9)	12 (60)
Smoking status		
Smoker	7 (31.8)	17 (85)
Non-smoker	15 (68.2)	3 (15)
Postoperative metastasis		
Yes	3 (13.6)	7 (35)
No	19 (86.4)	13 (65)
Median follow-up (months)	75.2	52.9

CEA, carcinoembryonic antigen; P-factor/LV-factor/V-factor, the status of tumor invasion into visceral pleura (P)/lymphatic vessels (LV)/veins (V).

incubated with Alexa 546 anti-rabbit IgG and Alexa 488 anti-mouse IgG (both 1:500) in darkness for 1 h, then washed with 0.075% Brij 35 in PBS in darkness and finally observed with 0.5 μg/ml DAPI for 1 min. The stained slides were analyzed under a laser scanning microscope (LSM 5 PASCAL; Carl Zeiss Inc., Germany).

Quantitative evaluation. Staining results were examined by two observers masked to patients' clinical information. Another reading by a third observer was needed to reach a consensus when there was a significant discrepancy between initial readings. At least 5 high-power fields and more than 2,000 cells were calculated in each case with a light microscope (Zeiss 2021-85; Carl Zeiss Inc.) at x400 magnification. Immunostaining results were evaluated by using a semi-quantitative scoring system according to the method described in the study by Ellinger *et al* (15). That is, the number of positive cancerous cells was estimated as follows (0, no positive cells; 1, 0> and ≤25% positive cells; 2, >25 and ≤50% positive cells; 3, >50 and ≤75% positive cells; and 4, >75 and ≤100% positive cells). These scores were multiplied with an intensity scale (0, negative; 1, weak; 2, moderate; and 3, intensive), and the final score ranged from 0-12.

Western blot analysis of H3K27me3. Western blot analysis was carried out as detailed previously (35). In brief, human lung cancer specimens and normal lung tissue were homogenized, and the lysates were centrifuged. Soluble proteins were separated on 10% SDS-PAGE gel (Daiichi Pure Chemical, Tokyo, Japan) with equal amounts (10 μg) of protein per lane. Separated proteins were electrophoretically transferred onto polyvinylidene difluoride (PVDF) membranes (Millipore), blocked with 10% non-fat milk in TBS (20 mM Tris buffer, pH 7.6, and 150 mM NaCl) for 1 h and then incubated overnight at 4˚C with rabbit polyclonal anti-H3 (Cell Signaling Technology, MA, USA) and H3K27me3 antibody. As a secondary antibody, HRP-goat anti-rabbit IgG was reacted for 1 h and then the bands were visualized with DAB, Ni, Co and H_2O_2.

In situ evaluation of DNA methylation. To evaluate the DNA methylation level of pathological slides of NSCLC at CCGG sites, histo-endonuclease-linked detection of methylation sites of DNA (HELMET) was performed (30). Paraffin sections were dewaxed and digested with 10 μg/ml of proteinase K in PBS at 37˚C for 15 min. Then the sections were incubated with TdT buffer (25 mM Tris-HCl buffer, pH 6.6, containing 0.2 M potassium cacodylate and 0.25 mg/ml BSA) alone at RT for 30 min. After incubation, the slides were reacted with 800 U/ml of TdT dissolved in TdT buffer containing 20 μM ddATP, 20 μM ddTTP, 1.5 mM $CoCl_2$ and 0.1 mM dithiothreitol at 37˚C for 2 h. After washing with PBS, the sections were fixed with freshly-prepared 4% PFA in PBS for 5 min and then rinsed with PBS. The non-methylated CCGG sites were digested at 37˚C for 2 h by 100 U/ml *Hpa*II dissolved in 10 mM Tris-HCl buffer (pH 7.5), containing 10 mM $MgCl_2$ and 1 mM dithiothreitol. The *Hpa*II-cut sites were labeled with biotin-16-dUTP by TdT reaction for 90 min. Then, the 3'-OH ends were blocked with a mixture of dideoxynucleotides by TdT, as described above, for 2 h. After fixation with 4% PFA in PBS, the methylated CCGG sites were digested at 37˚C for 2 h by 100 U/ml *Msp*I dissolved in Tris-HCl buffer (pH 7.9), containing 10 mM $MgCl_2$, 0.5 mM dithiothreitol,

Table II. List of antibodies used in immunohistochemistry.

Antibody	Working dilution/concentration	Manufacturer
Polyclonal, rabbit anti-human H3K27me3	1:200	Cell Signaling Technology, MA, USA
Monoclonal, rabbit anti-human EZH2	1:400	Cell Signaling Technology
Monoclonal, mouse anti-human PCNA (clone: PC10)	1:400	DakoCytomation, Glostrup, Denmark
HRP-conjugated goat anti-rabbit/mouse IgG	1:200	Millipore Co., CA, USA
Normal goat IgG	1:20	Sigma Chemical Co., MO, USA
Alexa 488 anti-mouse/Alexa546 anti-rabbit	1:500	Invitrogen Co., CA, USA
FITC-labeled goat anti-biotin	1:100	Vector Laboratories, CA, USA
Rhodamine-labeled sheep anti-digoxigenin	1:100	Roche Diagnostics, Mannheim, Germany

66 mM potassium acetate, and 0.1% BSA. The *Msp*I-cut sites were then labeled with digoxigenin-11-dUTP by TdT reaction for 90 min. Finally, the sections were incubated with a mixture of 500 μg/ml normal goat IgG and normal sheep IgG in 5% BSA/PBS for 1 h, and then visualized by FITC-labeled goat anti-biotin and rhodamine-labeled sheep anti-digoxigenin. The nuclei were stained with 0.5 μg/ml DAPI for 1 min.

Statistical analysis. The X-tile software program (Version 3.6.1; Yale University School of Medicine, New Haven, CT, USA) as described previously (36) was used to determine the best threshold value of H3K27me3 for classifying samples into groups of high and low expression. The SPSS 18.0 statistical software package (SPSS Inc, Chicago, IL, USA) was employed for all analyses. The association between tested markers and different clinicopathological characteristics of the patients, including age, gender, tissue type, tumor differentiation, P-factor, LV-factor, V-factor, smoking status, relapse, postoperative metastasis and CEA level were evaluated by Pearson's χ^2 or Fisher's exact test as appropriate. The Kaplan-Meier method with log-rank test was used for estimating probability of overall survival. The Cox proportional hazard model was used to evaluate the association between various markers and patient's survival. Univariate and multivariate analyses were determined by Cox regression. A p-value <0.05 was considered statistically significant.

Results

Clinicopathological data of patients. As shown in Table I, the diagnosis of the 5 normal lung specimens was identically pneumothorax. Three females and 2 males were included, with an average age of 67.6 years. The cancer patient population included 27 males and 15 females and had a mean age of 69 years. By histological classification, 20 cases were squamous cell carcinoma and 22 were adenocarcinoma. Of the 22 cases of adenocarcinoma, 13 patients had well-differentiated tumor, 6 had moderately- and 3 had poorly-differentiated tumor. In the 20 cases of squamous cell carcinoma, the well-, moderately- and poorly-differentiated numbers were 3, 9 and 8, respectively. All cases were TNM stage I and lymph node negative. Postoperative follow-up data were available in all cases, and the median follow-up duration in adenocarcinoma and squamous cell carcinoma groups were 75.2 months and 52.9 months, respectively.

Trimethylation level of histone H3 at lysine 27 in normal lung and NSCLC tissues. Either in normal lung or NSCLC tissues, H3K27me3 was localized predominantly in the nuclei (Fig. 1). Specificity of the antibody for H3K27me3 was determined by western blot analysis (Fig. 2H). Calculated staining score of immunopositive cells ranged from 0 to 12 in all tested tissues. According to the X-tile plots (Fig. 2D-F), we categorized the samples into low (IHC score ≤3) and high (IHC score >3) expression subgroups based on a cut-point determined by X-tile software related to survival status ((Fig. 2F, P<0.05). As shown in Fig. 2A, high expression of H3K27me3 was observed in all 5 (100%) normal lung tissues, whereas in cancer tissues, high methylation level of H3K27 was found in 18 (81.8%) adenocarcinomas and 6 (30%) squamous cell carcinomas (P<0.01). The staining score of H3K27me3 was significantly higher in normal lung tissue compared to those of adenocarcinoma and squamous cell carcinoma (11.2±0.8, 7.55±0.77 and 3.55±0.61, respectively, P<0.05, Figs. 1 and 2A). In addition, a positive relationship between tumor differentiation and H3K27me3 expression was found (Figs. 1, 2B and C). In both cancer subtypes, higher positive staining score was correlated with better cellular differentiation (P<0.01). In the adenocarcinoma subgroup, staining scores for well-, moderately- and poorly-differentiated NSCLC samples were 8.69±1.00, 7.00±1.24 and 3.67±1.20, respectively (P<0.01). In the squamous cell carcinoma subgroup, their staining scores were 8.00, 2.78±0.70 and 2.75±0.82, respectively (P<0.01).

Correlation of H3K27me3 expression with clinicopathological parameters. To determine the correlation of H3K27me3 expression and clinicopathological parameters, and to determine its prognostic impact, χ^2 analyses together with univariate, multivariate and Kaplan-Meier survival analyses of cumulative survival analysis were performed. Correlation analyses (Table III) revealed that H3K27me3 expression was significantly associated with non-SCC histology (P=0.001), better cellular differentiation (P=0.002), non-smoking status (P=0.019), low EZH2 expression (P=0.038), high methylation level at CCGG sites (P=0.049) and tumor-specific survival after resection of primary tumors (P<0.01 by log-rank test, Fig. 2G). Kaplan-Meier survival analysis revealed

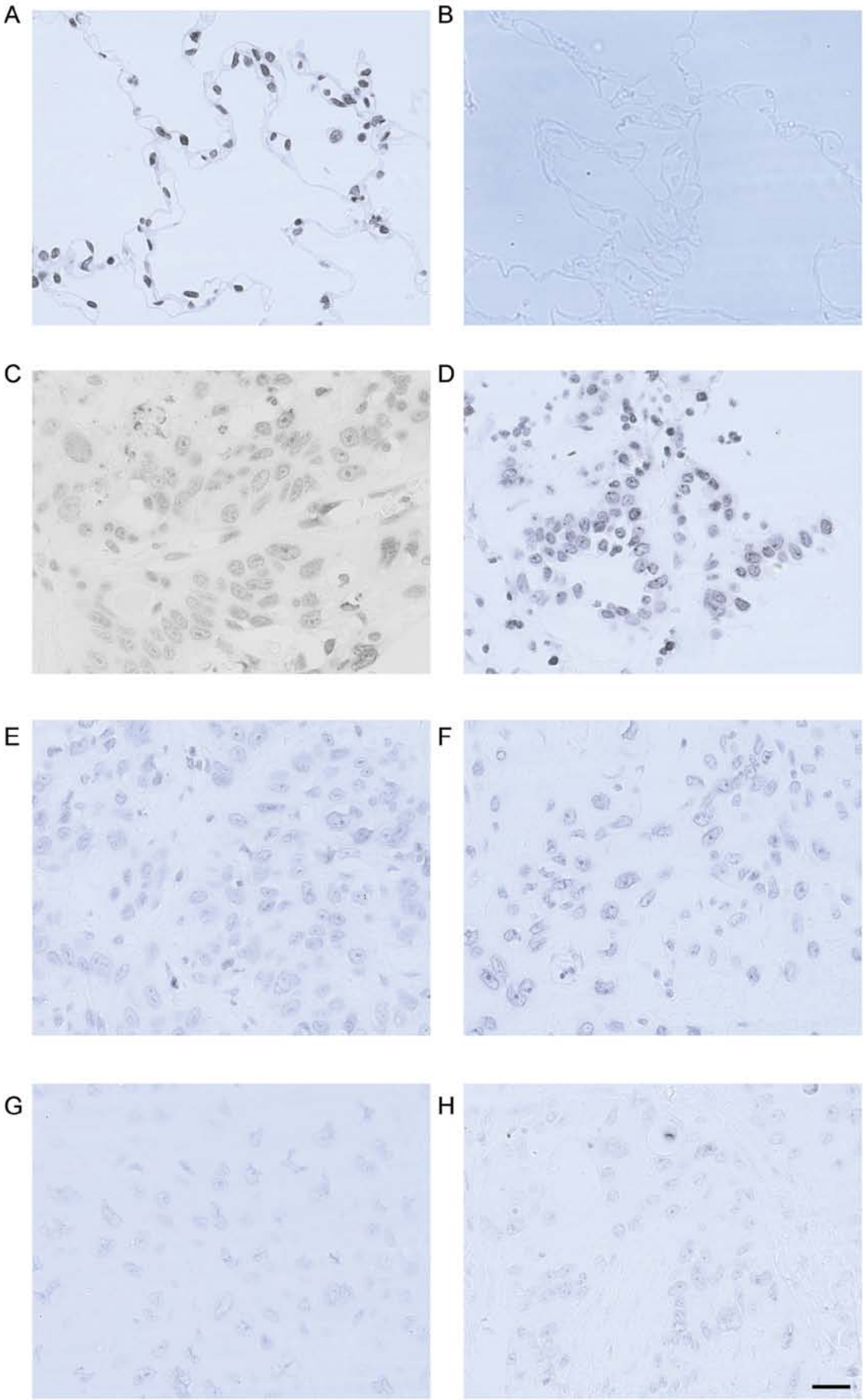

Figure 1. Immunohistochemical staining for H3K27me3 in different lung tissues and its relationship with overall survival. (A) Strong expression of H3K27me3 in normal lung tissue; (B) negative control; scale bar, 20 μm. (C, E and G) H3K27me3 expression varied obviously in well, moderate and poor differentiation of squamous cell carcinoma. (D, F and H) H3K27me3 expression varied obviously in well, moderate and poor differentiation of adenocarcinoma, which decreased as differentiation level reduced.

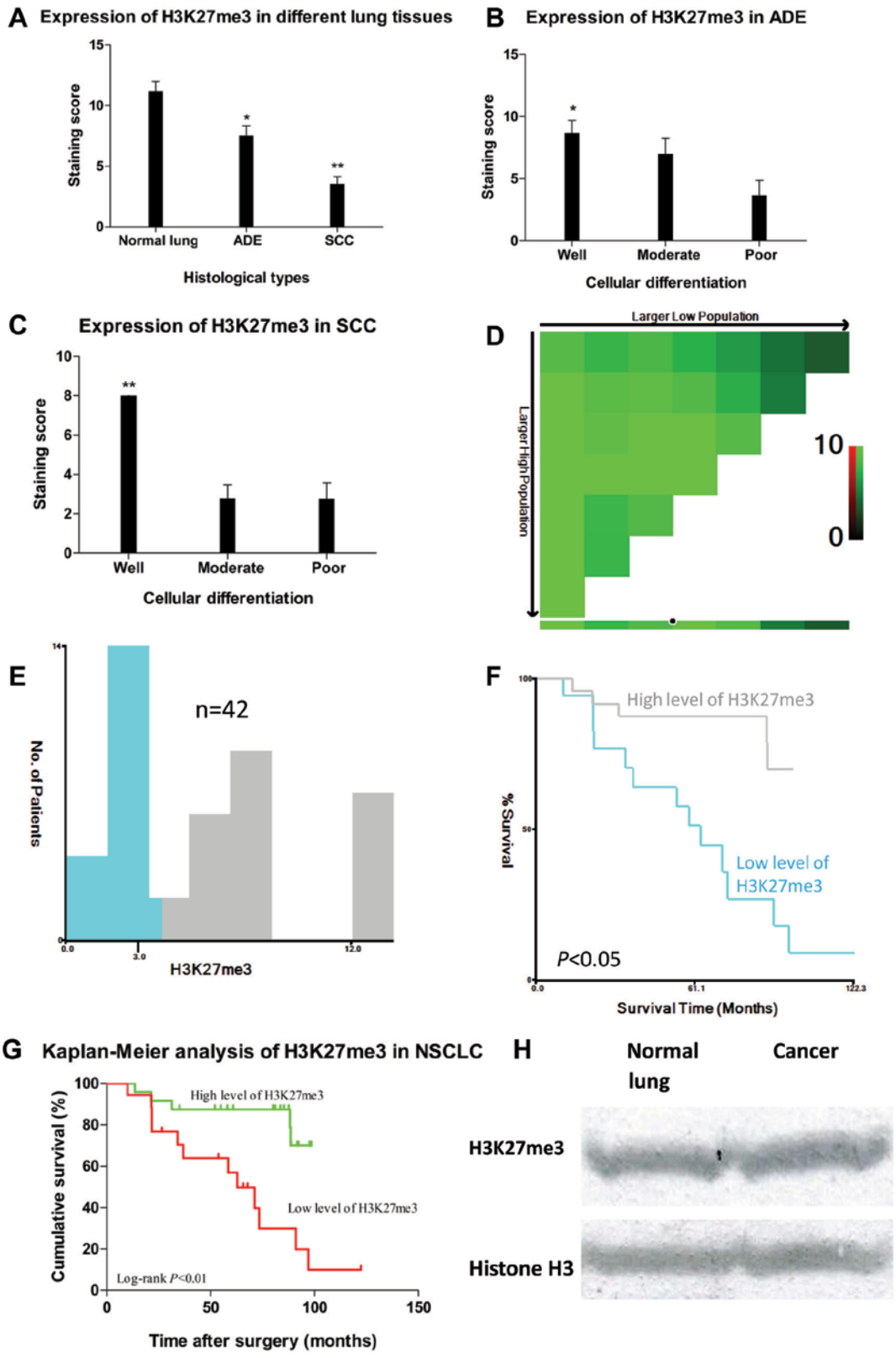

Figure 2. (A) H3K27me3 expression differed in different lung tissues, *P<0.05 and **P<0.01 compared to normal lung; error bars, SD of mean. (B) In ADE, H3K27me3 expression reduced markedly as differentiation decreased, *P<0.05 compared to poor differentiation. (C) In SCC, H3K27me3 expression reduced markedly as differentiation decreased, **P<0.01 compared to moderate or poor differentiation. (D) X-tile plots of H3K27me3 expression for optimal cut-point (3, P<0.05), which is demarcated by the circle (black with white border). (E) The cut-point was used to separate low H3K27me3 expression (blue) from high H3K27me3 expression (gray) in the expression frequency histogram of the whole sample set. (F) Kaplan-Meier curve for testing the survival of sample subsets defined by H3K27me3 expression below 3 (green line) and above 3 (gray line). (G) Kaplan-Meier curves of OS in different levels of H3K27me3 expression in NSCLC patients. High expression of H3K27me3 (green line) was associated with better prognostic outcome and longer disease-free survival time while low expression of H3K27me3 (red line) with worse prognosis and shorter DFS/OS, P<0.05. (H) To determine the specificity of H3K27me3 antibody, western blot analysis (10 μg protein/lane) were performed to detect H3K27me3 expression in both normal lung tissue (upper left panel) and lung adenocarcinoma (upper right panel, well differentiation), and histone H3 expression was used as internal control (lower panel).

Table III. Association of H3K27me3, EZH2 expression and DNA methylation level at CCGG sites with clinicopathologic parameters in NSCLC patients.

	H3K27me3				EZH2				DNA methylation			
Variables	All cases	H	L	P-value	All cases	H	L	P-value	All cases	H	L	P-value
Age[a] (y.o.)				0.857				0.653				0.245
≤69	18	10	8		18	7	11		24	9	15	
>69	24	14	10		24	11	13		18	10	8	
Gender				0.114				0.026				0.152
Male	27	13	14		27	15	12		27	10	17	
Female	15	11	4		15	3	12		15	9	6	
Tissue type				0.001				0.000				0.059
ADE	22	18	4		22	3	19		22	13	9	
SCC	20	6	14		20	15	5		20	6	14	
Differentiation				0.002				0.067				0.261
Well	16	14	2		16	4	12		16	9	7	
Moderate/poor	26	10	16		26	14	12		26	10	16	
P-factor[b]				1.000				1.000				0.452
Yes	1	1	0		1	0	1		1	1	0	
No	41	23	18		41	18	23		41	18	23	
LV-factor[b]				1.000				1.000				0.180
Yes	31	18	13		31	13	18		31	12	19	
No	11	6	5		11	5	6		11	7	4	
V-factor				0.150				0.038				0.049
Yes	18	8	10		18	11	7		18	5	13	
No	24	16	8		24	7	17		24	14	10	
Smoking status				0.019				0.019				0.016
Smoker	24	10	14		24	14	10		24	7	17	
Non-smoker	18	14	4		18	4	14		18	12	6	
Relapse[b]				0.010				0.720				1.000
Yes	10	2	8		10	5	5		10	4	6	
No	32	22	10		32	13	19		32	15	17	
Postoperative metastasis[b]				0.281				0.281				0.305
Yes	10	4	6		10	6	4		10	3	7	
No	32	20	12		22	12	20		32	16	16	
CEA[b] (ng/ml)				0.567				0.071				0.239
≤5	39	23	16		39	15	24		39	19	20	
>5	3	1	2		3	3	0		3	0	3	
EZH2[c]				0.038								0.049
≤3.7	24	17	7						24	14	10	
>3.7	18	7	11						18	5	13	
H3K27me3[d]								0.038				0.049
≤3					18	11	7		18	5	13	
>3					24	7	17		24	14	10	
DNA methylation[c]				0.049				0.049				
≤2.64	23	10	13		23	13	10					
>2.64	19	14	5		19	5	14					
PCNA[b]				0.214				0.029				0.384
≤10%	6	5	1		6	0	6		6	4	2	
>10%	36	19	17		36	18	18		36	15	21	

H, high expression/high CCGG sites methylation; L, low expression/low CCGG sites methylation; ADE, adenocarcinoma; SCC, squamous cell carcinoma; CEA, carcinoembryonic antigen; PCNA, proliferating cell nulear antigen; [a]mean age; [b]Fisher's exact tests (two-sided); χ^2 test for all the other analyses; [c]mean score/ratio; [d]cut-point determined by X-tile software.

Table IV. Univariate and multivariate analyses of factors associated with OS.

Variables	Hazard ratio (95% confidential interval, CI)	P-value
Univariate analysis		
Age (≤69 vs. >69)	1.248 (0.480-3.249)	0.649
Gender (male vs. female)	0.461 (0.161-1.319)	0.149
Tissue type (ADE vs. SCC)	0.276 (0.102-0.744)	0.011
Differentiation (well vs. moderate/poor)	0.338 (0.109-1.048)	0.060
P-factor (yes vs. no)	21.193 (0.000-1.031E7)	0.648
LV-factor (yes vs. no)	0.921 (0.323-2.622)	0.877
V-factor (yes vs. no)	0.573 (0.227-1.448)	0.239
Smoking status (smoker vs. non-smoker)	0.131 (0.036-0.472)	0.002
Relapse (yes vs. no)	0.134 (0.050-0.359)	0.000
Postoperative metastasis (yes vs. no)	0.115 (0.041-0.322)	0.000
Serum CEA level (ng/ml) (≤5 vs. >5)	0.043 (0.000-174.939)	0.458
H3K27me3 (high vs. low)	0.187 (0.066-0.531)	0.002
EZH2 (high vs. low)	1.975 (0.775-5.031)	0.154
DNA methylation (high vs. low)	0.441 (0.165-1.176)	0.102
PCNA (high vs. low)	0.755 (0.286-1.991)	0.569
Multivariate analysis		
Postoperative metastasis (yes vs. no)	0.115 (0.041-0.322)	0.000
H3K27me3 (high vs. low)	0.205 (0.068-0.614)	0.005

that patients with higher H3K27me3 expression in tumors showed longer disease-free survival in contrast to those with low expression. Univariate analysis revealed associations between poor prognosis in NSCLC patients and several factors, including low H3K27me3 expression (P=0.002), histologic type (non-ADE, P=0.011), smoking status (smoker, P=0.002), relapse (P<0.01), and postoperative metastasis (P<0.01, Table IV). Using a Cox proportional hazard regression analysis, we found that expression of H3K27me together with postoperative metastasis were independent predictors associated with prognostic outcome (Table IV).

Expression of EZH2 in lung tissues and its correlation with clinicopathological parameters. As shown in Fig. 3 (right panel), EZH2 was localized predominantly in nuclei, although occasionally it could be seen in the cytoplasm as background. In contrast with H3K27me3, no EZH2 staining was found in any of the 5 normal lung samples, and the staining for EZH2 in SCC was generally more intense than that of ADE (5.40±0.71 vs. 2.18±0.54, P<0.01, Fig. 3B, D, F and G). Of 22 adenocarcinomas, 3 cases (13.6%) were defined as high expression. While in squamous cell carcinoma group, 15 out of 20 cases (75%) were considered as high expression (Fig. 3G). χ^2 analyses demonstrated that when related to clinicopathological data (Table III), expression of EZH2 in NSCLC patients was found to be significantly associated with male gender (P=0.026), non-ADE histology (P<0.01), smoking status (P=0.019), low H3K27me3 expression (P=0.038), invasion into veins (V-factor, P=0.038), low methylation level at CCGG sites (P=0.049) and high PCNA percentage (P=0.029). It should be noted that the expression of EZH2 was correlated with lower level of H3K27 methylation while with enhanced PCNA expression, indicating its positive correlation with cell proliferating activity (Table III, Figs. 3A-F and 4). The reciprocal expression pattern of EZH2 and H3K27me3 in NSCLC was also confirmed immunohistochemically in mirror sections. As shown in Fig. 5, in lung adenocarcinoma (upper panel), the cells heavily stained for H3K27me3 were essentially negative or weak for EZH2 staining. In lung squamous cell carcinoma (lower panel), the expression of H3K27me3 seemed generally weaker than that of adenocarcinoma, however, identical cells with negative or weak staining of H3K27me3 were found with high level expression of EZH2. Both correlation analysis (Table III) and immunofluorescence double staining for EZH2 and PCNA (Fig. 4) confirmed that PCNA index was positively correlated with EZH2 expression. In contrast, neither univariate nor multivariate analysis indicated that EZH2 was an independent prognostic factor for surgically treated NSCLC patients enrolled in this study (P=0.720).

DNA methylation level at CCGG sites and its relation with clinicopathological parameters. As shown in Figs. 6 and 7, CCGG sites in cancer cells were generally hypermethylated, compared to that of normal cells. Although no correlation was found between DNA methylation level at CCGG sites and DFS/OS, we found that higher DNA methylation level at CCGG sites in NSCLC patients was significantly associated with less pulmonary vein invasion (V-factor, P=0.049), non-smoking status (P=0.016), low EZH2 expression (P=0.049) and high H3K27me3 expression (P=0.049) (Table III). Although the expression of H3K27me3 was correlated with differentiation status, and DNA methylation level at CCGG sites was correlated with the methylation level of H3K27 positively, no correlation between DNA methylation and differentiation level was found (P=0.261).

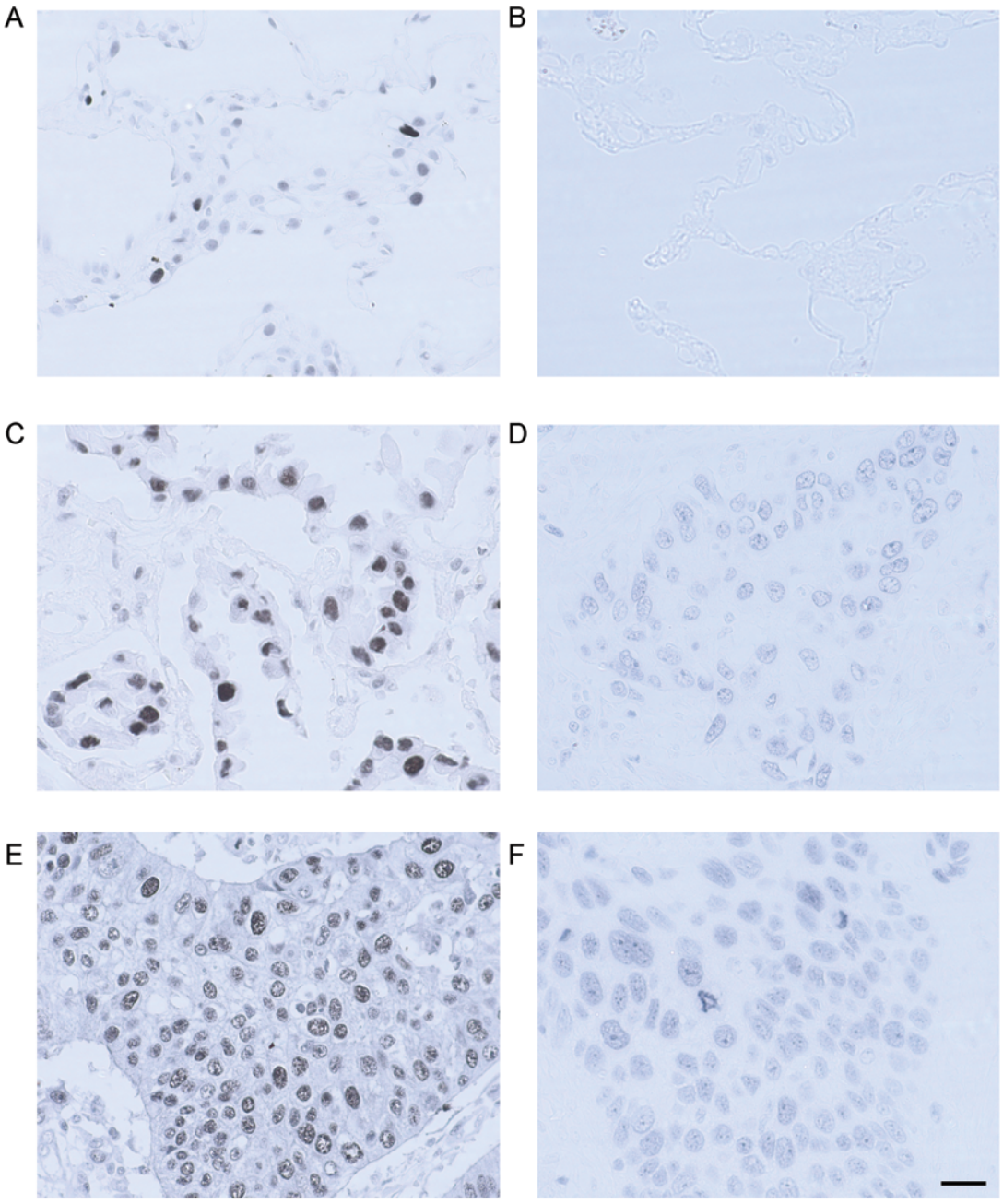

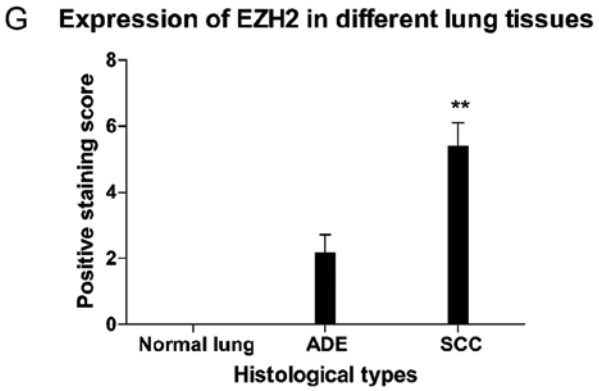

Figure 3. Correlation of expressions of EZH2 and PCNA in different lung tissues. Expression patterns of (A) PCNA and (B) EZH2 in normal lung (upper panel), adenocarcinoma (C and D, middle panel) and squamous cell carcinoma (E and F, lower panel) detected by IHC. Expression of PCNA was collateral with that of EZH2 in NSCLC tissues; scale bar, 20 μm. (G) Expression of EZH2 differed in different lung tissues; **P<0.01 compared to normal lung and ADE; error bars, SD of mean.

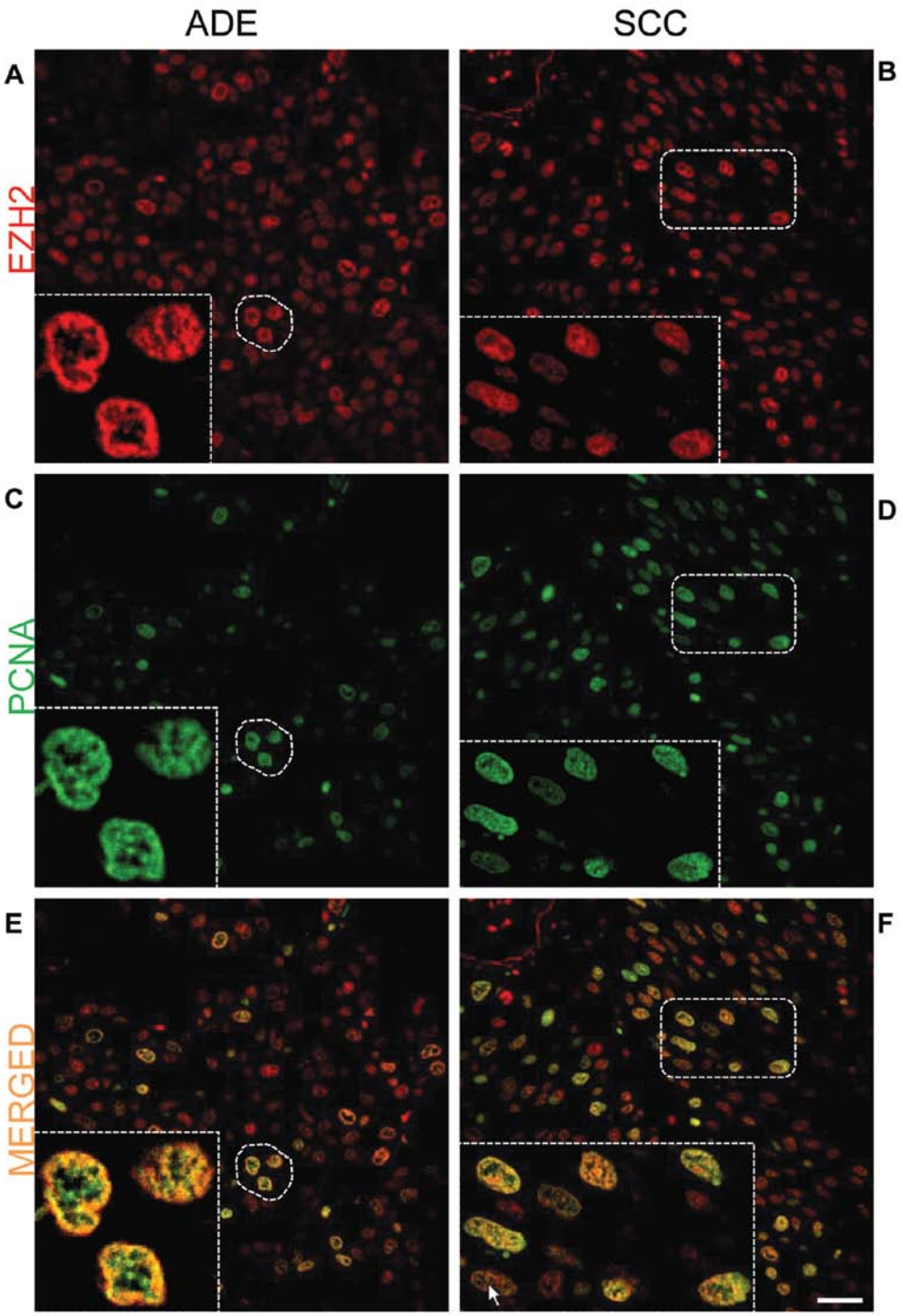

Figure 4. Immunofluorescence double staining for EZH2 (rhodamine) and PCNA (FITC) in adenocarcinoma (left panel) and squamous cell carcinoma (right panel). Highlighted dotted area indicates that cancerous cells with high expression of EZH2 also exhibit high expression of PCNA, demonstrating their high level of cellular proliferation. Scale bar, 20 μm.

Discussion

In the present study, we investigated the prognostic value of H3K27me3 and EZH2 expression in human lung cancer immunohistochemically, and found that, in comparison to normal lung tissue, the level of H3K27me3 was significantly downregulated in both ADE and SCC tissues of early-staged NSCLC. Furthermore, in each cancer subtype, the level of H3K27me3 was antiparallel with the cellular differentiation level, and the decrease in H3K27me3 was significantly correlated with tumor relapse and shorter overall survival, strongly demonstrating that the level of H3K27me3 is a new epigenetic marker in lung cancers. In contrast, although EZH2 is known to catalyze trimethylation of H3K27, the expression of EZH2 in it was not significantly correlated with lung carcinogenesis.

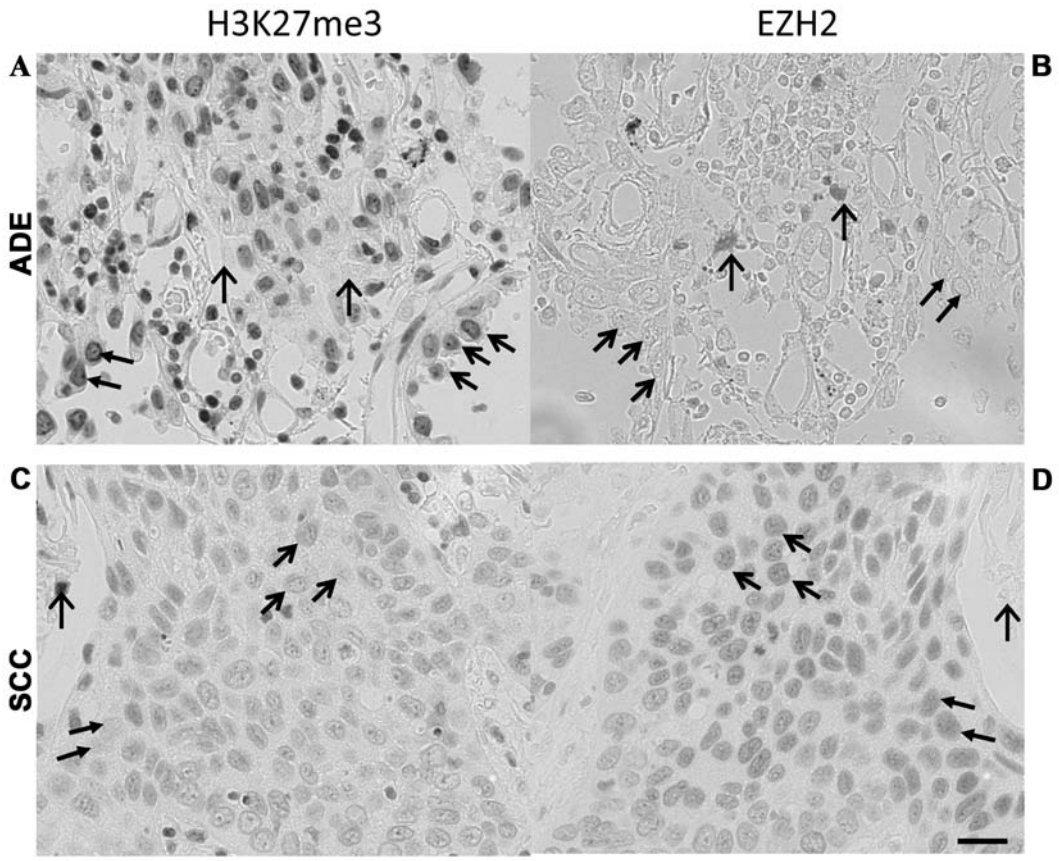

Figure 5. Immunohistochemical staining for H3K27me3 (left panel) and EZH2 (right panel) in mirror sections of ADE (upper panel) and SCC (lower panel), demonstrating the reciprocal correlation between expression of H3K27me3 and EZH2. That is, NSCLC cells with high H3K27me3 expression exhibited low or negative expression of EZH2, and vice versa. Some cells with heavy staining of H3K27me3 are lymphocytes rather than cancer cells. The same type of arrows indicate the same cell type; scale bar, 20 μm.

With regard to the prognostic impact of H3K27me3 in various human cancers, it was reported that overexpression of H3K27me3 was linked to more malignant behavior and worse prognosis in patients with prostate (15), esophageal (17), nasopharyngeal (18) and hepatocellular carcinomas (14). On the other hand, in breast, ovarian and pancreatic cancers (5) and renal cell carcinoma (37), reduced expression of H3K27me3 was associated with worse prognosis. In human NSCLCs, however, we have found that a lower level of H3K27me3 was associated with higher tumor invasiveness and/or poorer disease-free survival (DFS) in this study. These contradictory findings may in part reflect that H3K27me3 marks different genes for silencing in different cell types. In the present study, we observed that low expression of H3K27me3 was a strong and independent predictor of poor cellular differentiation and shortened cancer-specific survival, as evidenced by univariate and multivariate analyses (Table IV). When the Cox regression model was constructed for the entire series, low H3K27me3 expression remained an independent predictive factor of recurrence and/or cancer death in NSCLC patients. To our knowledge, our data presented here demonstrated for the first time a direct association of expression of H3K27me3 with clinical outcome with NSCLCs. As H3K27me3 serves as an epigenetic mark mediating silencing and represses target gene expression, loss of it may result in reactivation of these silenced genes, such as some oncogenes, and therefore contributing to tumorigenesis or cancer progression.

EZH2 is involved in PRC2-directed gene silencing through the formation of H3K27me3 as an epigenetic marker. It was reported that EZH2 was found to be overexpressed at both mRNA and protein levels in NSCLC and bladder cancer, and correlated with invasiveness, increased proliferation and poor outcome (20,21). In colorectal cancer, EZH2 overexpression indicated a good prognosis, in contrast to the poor prognosis associated with EZH2 overexpression in NSCLCs (20). In the current study, we found that the higher expression of EZH2 in NSCLC patients was significantly associated with various clinicopathological parameters including PCNA labeling index, which was consistent with the findings of Takawa *et al* (20), while we failed to confirm the significant correlation with poor prognosis (P=0.154). Further study with a greater number of specimens is needed.

In addition, we found that the expression of H3K27me3 was reversely correlated with that of EZH2 in NSCLC (Table III and Fig. 5). Similar findings have been recently reported by Holm *et al* (38) in breast cancer. Previous studies indicated that the polycomb group protein EZH2 directly methylated DNA in either normal (39) or cancerous (11) tissues, and might result in the inhibition of target gene expression through its methylation, also overexpression of EZH2 promoted formation of a different PRC complex, the PRC4, and exhibited differential

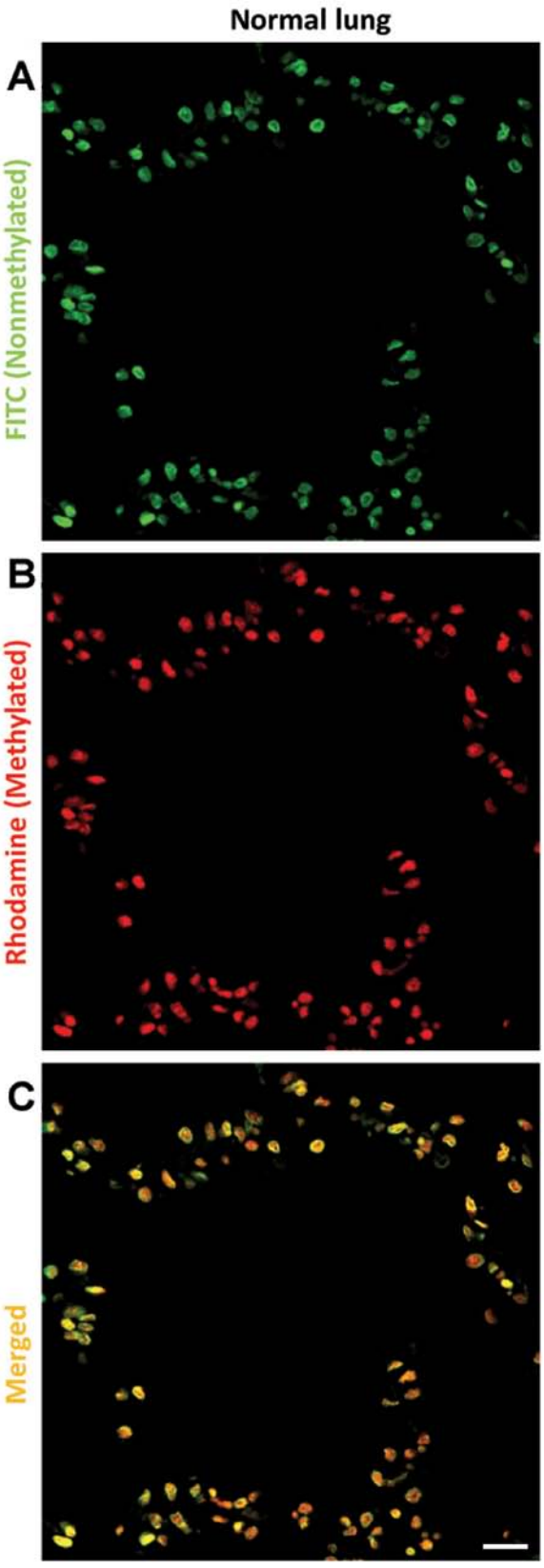

Figure 6. Simultaneous localization of non-methylated and methylated CCGG sequences by HELMET in paraffin-embedded sections of normal lung. The paraffin-embedded section was blocked with a dideoxynucleotide mixture by TdT and then the Hpa II cutting sites were labeled with biotin-16-dUTP. After dideoxynucleotide blockade, Msp I cutting sites were labeled with digoxigenin-11-dUTP and both haptens were visualized with (A) FITC anti-biotin and (B) rhodamine anti-digoxigenin, respectively. Merged images are shown in (C). In normal lung tissue, both non-methylated and methylated CCGG sequences were evenly distributed within the nuclei.

histone substrate specificities (40). Loss of H3K27me3 in tumor might reflect the formation of the new PRC complex to modify other histone residues. Since EZH2 methyltransferase activity requires its association with other PRC components, it has been proposed that overexpression of EZH2 may result in the disruption of the integrity of the PRC complexes or may form new PRC complexes (41,42), and thus the methyltransferase activity toward H3K27 may be changed.

It is clear that histone methylation marks do not act alone, but in a coordinated manner with other epigenetic modifications (4). DNA methylation principally occurs at cytosine residues located in dinucleotide CpG sites (43). CpG dinucleotides are statistically under-represented in the genome but are found to be concentrated in CG-rich regions termed CpG islands that frequently coincide with promoter or gene regulatory regions (3). Global hypomethylation appears to be an early event for colon and breast cancer as well as chronic lymphacytic leukemia (CLL) (44). In the present study, we evaluated the DNA methylation level at CCGG sites by means of HELMET, indicating that cancerous tissues were relatively hypermethylated in DNA at CCGG sites in contrast to that of normal lung tissue. This result is consistent with previous finding, that gene hypermethylation is an early event in the process of tumorigenesis of lung cancer (45). We also found that higher DNA methylation level at CCGG sites were statistically correlated with less chance of venous invasion, non-smoking status, lower expression of EZH2 and higher expression of H3K27me3 as well, although no significance of correlation with overall survival was found. This finding might still suggest that hypermethylation at CCGG sites contributes to better prognosis in NSCLC patients, because those factors were more or less affecting the outcome of NSCLC patients. On the other hand, Lin *et al* (46) have reported that hypermethylation in CpG was correlated with poor prognosis in NSCLC, contrary to our findings. Although the reason for this discrepancy is not known, the genes that were hypermethylated in the studies might be different. Since DNA methylation in cancer was mainly targeted to polycomb-regulated genes and a very high percentage of the methylated genes was pre-marked with trimethylated H3K27 in addition to other polycomb components (10), further study is needed to clarify which gene is involved and whether or not methylation of H3K27 also plays a role in the interaction with this hypermethylation.

Some limitations of this research should be noted. First of all, the dataset was small and as a result the statistical power would be somewhat limited. Further study with larger number of samples is necessary to validate the present results. Although the number of specimens used here was limited, we did achieve some significant indications, showing that high expression of H3K27me3 was correlated with longer disease-free survival. Secondly, all the cases involved in this study were patients of TNM stage I. Although chemotherapy or radiotherapy would be used after progression had been proved, the contribution of other therapies to overall survival had not been taken into account in the survival analysis, for surgery was considered the key therapy for patients at this stage, and thus would probably lead to some bias.

In conclusion, our study indicated that high expression of H3K27me3 was associated with clinicopathological parameters

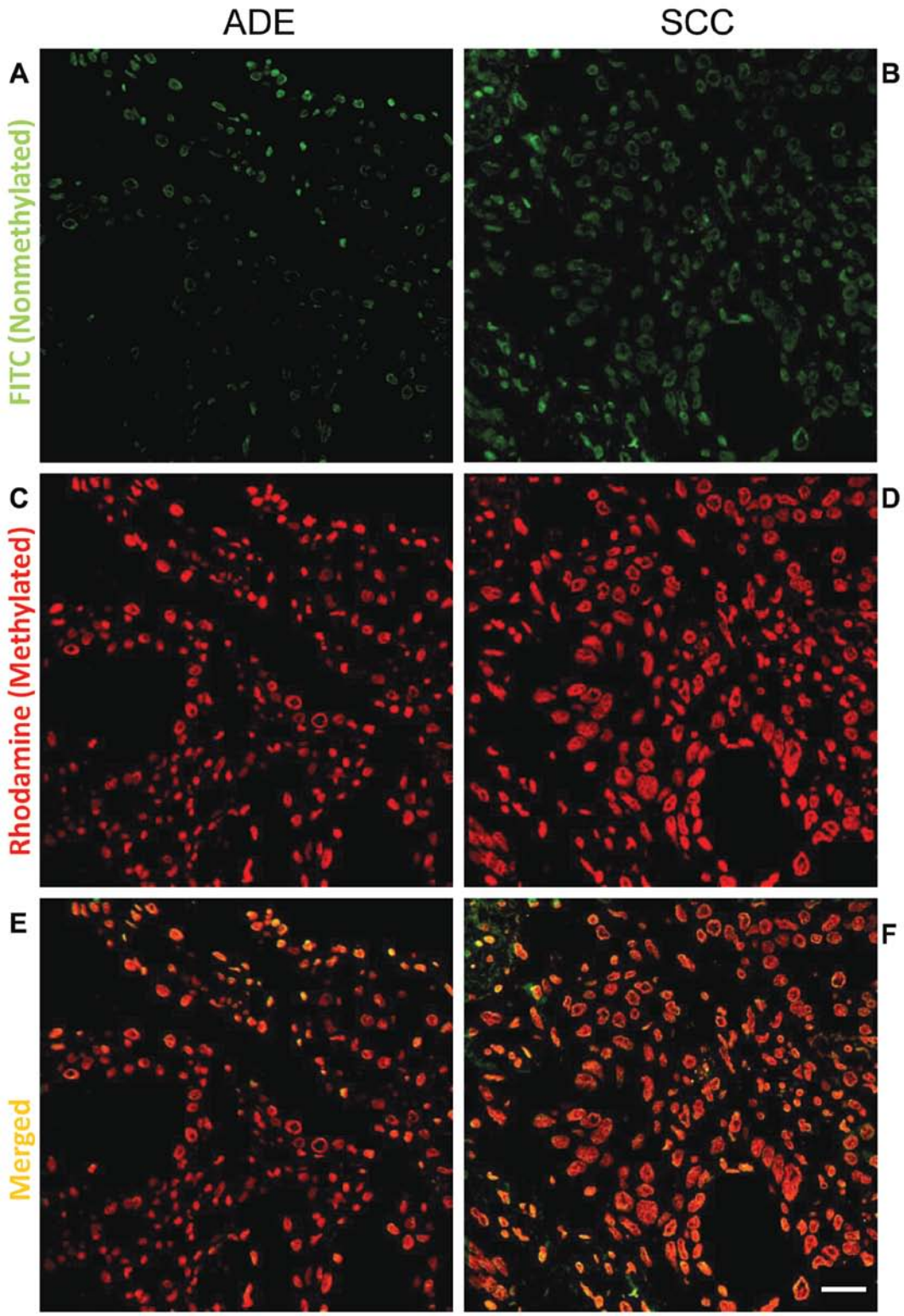

Figure 7. Simultaneous localization of non-methylated and methylated CCGG sequences by HELMET in paraffin-embedded sections of ADE (left panel) and SCC (right panel). In contrast to normal lung tissue, hypermethylation was observed in both cancer tissue types. Within two types of NSCLC, higher methylation ratio in adenocarcinoma (left panel) was observed while relatively lower methylation ratio was found in squamous cell carcinoma (right panel), scale bar, 20 μm.

and correlated with better outcome in NSCLC patients as well. Thus H3K27me3 can be used as a good marker, enabling us to predict the prognosis of NSCLC patients, and to carry out a more intensive follow-up according to H3K27me3 expression status in resected specimens.

Acknowledgements

This study was supported in part by a Grant-in-Aid for Scientific Research from the Japan Society for the Promotion of Science (no. 18390060 to T.K.).

References

1. Jemal A, Bray F, Center MM, Ferlay J, Ward E and Forman D: Global cancer statistics. CA Cancer J Clin 61: 69-90, 2011.
2. Lund AH and van Lohuizen M: Epigenetics and cancer. Genes Dev 18: 2315-2335, 2004.
3. Taniguchi H, Yamamoto H, Akutsu N, *et al*: Transcriptional silencing of hedgehog-interacting protein by CpG hypermethylation and chromatic structure in human gastrointestinal cancer. J Pathol 213: 131-139, 2007.
4. Zhang C, Li H, Zhou G, *et al*: Transcriptional silencing of the TMS1/ASC tumour suppressor gene by an epigenetic mechanism in hepatocellular carcinoma cells. J Pathol 212: 134-142, 2007.
5. Wei Y, Xia W, Zhang Z, *et al*: Loss of trimethylation at lysine 27 of histone H3 is a predictor of poor outcome in breast, ovarian, and pancreatic cancers. Mol Carcinog 47: 701-706, 2008.
6. Mitani Y, Oue N, Hamai Y, *et al*: Histone H3 acetylation is associated with reduced p21(WAF1/CIP1) expression by gastric carcinoma. J Pathol 205: 65-73, 2005.
7. Kouzarides T: Chromatin modifications and their function. Cell 128: 693-705, 2007.
8. Prystowsky MB, Adomako A, Smith RV, *et al*: The histone deacetylase inhibitor LBH589 inhibits expression of mitotic genes causing G2/M arrest and cell death in head and neck squamous cell carcinoma cell lines. J Pathol 218: 467-477, 2009.
9. Ohm JE, McGarvey KM, Yu X, *et al*: A stem cell-like chromatin pattern may predispose tumor suppressor genes to DNA hypermethylation and heritable silencing. Nat Genet 39: 237-242, 2007.
10. Schlesinger Y, Straussman R, Keshet I, *et al*: Polycomb-mediated methylation on Lys27 of histone H3 pre-marks genes for de novo methylation in cancer. Nat Genet 39: 232-236, 2007.
11. Vire E, Brenner C, Deplus R, *et al*: The Polycomb group protein EZH2 directly controls DNA methylation. Nature 439: 871-874, 2006.
12. Karlic R, Chung HR, Lasserre J, Vlahovicek K and Vingron M: Histone modification levels are predictive for gene expression. Proc Natl Acad Sci USA 107: 2926-2931, 2010.
13. Yoo KH and Hennighausen L: EZH2 methyltransferase and H3K27 methylation in breast cancer. Int J Biol Sci 8: 59-65, 2012.
14. Cai MY, Hou JH, Rao HL, *et al*: High expression of H3K27me3 in human hepatocellular carcinomas correlates closely with vascular invasion and predicts worse prognosis in patients. Mol Med 17: 12-20, 2011.
15. Ellinger J, Kahl P, von der Gathen J, *et al*: Global histone H3K27 methylation levels are different in localized and metastatic prostate cancer. Cancer Invest 30: 92-97, 2012.
16. Anderton JA, Bose S, Vockerodt M, *et al*: The H3K27me3 demethylase, KDM6B, is induced by Epstein-Barr virus and over-expressed in Hodgkin's lymphoma. Oncogene 30: 2037-2043, 2011.
17. Tzao C, Tung HJ, Jin JS, *et al*: Prognostic significance of global histone modifications in resected squamous cell carcinoma of the esophagus. Mod Pathol 22: 252-260, 2009.
18. Cai MY, Tong ZT, Zhu W, *et al*: H3K27me3 protein is a promising predictive biomarker of patients' survival and chemoradioresistance in human nasopharyngeal carcinoma. Mol Med 17: 1137-1145, 2011.
19. Chase A and Cross NC: Aberrations of EZH2 in cancer. Clin Cancer Res 17: 2613-2618, 2011.
20. Takawa M, Masuda K, Kunizaki M, *et al*: Validation of the histone methyltransferase EZH2 as a therapeutic target for various types of human cancer and as a prognostic marker. Cancer Sci 102: 1298-1305, 2011.
21. Huqun, Ishikawa R, Zhang J, *et al*: Enhancer of zeste homolog 2 is a novel prognostic biomarker in nonsmall cell lung cancer. Cancer 118: 1599-1606, 2012.
22. Gong Y, Huo L, Liu P, *et al*: Polycomb group protein EZH2 is frequently expressed in inflammatory breast cancer and is predictive of worse clinical outcome. Cancer 117: 5476-5484, 2011.
23. Kleer CG, Cao Q, Varambally S, *et al*: EZH2 is a marker of aggressive breast cancer and promotes neoplastic transformation of breast epithelial cells. Proc Natl Acad Sci USA 100: 11606-11611, 2003.
24. Chang CJ, Yang JY, Xia W, *et al*: EZH2 promotes expansion of breast tumor initiating cells through activation of RAF1-beta-catenin signaling. Cancer Cell 19: 86-100, 2011.
25. Kunju LP, Cookingham C, Toy KA, Chen W, Sabel MS and Kleer CG: EZH2 and ALDH-1 mark breast epithelium at risk for breast cancer development. Mod Pathol 24: 786-793, 2011.
26. Alford SH, Toy K, Merajver SD and Kleer CG: Increased risk for distant metastasis in patients with familial early-stage breast cancer and high EZH2 expression. Breast Cancer Res Treat 132: 429-437, 2012.
27. Bachmann IM, Halvorsen OJ, Collett K, *et al*: EZH2 expression is associated with high proliferation rate and aggressive tumor subgroups in cutaneous melanoma and cancers of the endometrium, prostate, and breast. J Clin Oncol 24: 268-273, 2006.
28. Fujii S, Fukamachi K, Tsuda H, Ito K, Ito Y and Ochiai A: RAS oncogenic signal upregulates EZH2 in pancreatic cancer. Biochem Biophys Res Commun 417: 1074-1079, 2012.
29. Guo J, Cai J, Yu L, Tang H, Chen C and Wang Z: EZH2 regulates expression of p57 and contributes to progression of ovarian cancer in vitro and in vivo. Cancer Sci 102: 530-539, 2011.
30. Koji T, Kondo S, Hishikawa Y, An S and Sato Y: In situ detection of methylated DNA by histo endonuclease-linked detection of methylated DNA sites: a new principle of analysis of DNA methylation. Histochem Cell Biol 130: 917-925, 2008.
31. An S, Hishikawa Y and Koji T: Induction of cell death in rat small intestine by ischemia reperfusion: differential roles of Fas/Fas ligand and Bcl-2/Bax systems depending upon cell types. Histochem Cell Biol 123: 249-261, 2005.
32. Shirendeb U, Hishikawa Y, Moriyama S, *et al*: Human papillomavirus infection and its possible correlation with p63 expression in cervical cancer in Japan, Mongolia, and Myanmar. Acta Histochem Cytochem 42: 181-190, 2009.
33. Song N, Liu J, An S, Nishino T, Hishikawa Y and Koji T: Immunohistochemical analysis of histone H3 modifications in germ cells during mouse spermatogenesis. Acta Histochem Cytochem 44: 183-190, 2011.
34. Adams JC: Heavy metal intensification of DAB-based HRP reaction product. J Histochem Cytochem 29: 775, 1981.
35. Yamayoshi T, Nagayasu T, Matsumoto K, Abo T, Hishikawa Y and Koji T: Expression of keratinocyte growth factor/fibroblast growth factor-7 and its receptor in human lung cancer: correlation with tumour proliferative activity and patient prognosis. J Pathol 204: 110-118, 2004.
36. Camp RL, Dolled-Filhart M and Rimm DL: X-tile: a new bio-informatics tool for biomarker assessment and outcome-based cut-point optimization. Clin Cancer Res 10: 7252-7259, 2004.
37. Rogenhofer S, Kahl P, Mertens C, *et al*: Global histone H3 lysine 27 (H3K27) methylation levels and their prognostic relevance in renal cell carcinoma. BJU Int 109: 459-465, 2012.
38. Holm K, Grabau D, Lovgren K, *et al*: Global H3K27 trimethylation and EZH2 abundance in breast tumor subtypes. Mol Oncol 6: 494-506, 2012.
39. Chen H, Tu SW and Hsieh JT: Down-regulation of human DAB2IP gene expression mediated by polycomb Ezh2 complex and histone deacetylase in prostate cancer. J Biol Chem 280: 22437-22444, 2005.
40. Kuzmichev A, Margueron R, Vaquero A, *et al*: Composition and histone substrates of polycomb repressive group complexes change during cellular differentiation. Proc Natl Acad Sci USA 102: 1859-1864, 2005.
41. Cao R and Zhang Y: The functions of E(Z)/EZH2-mediated methylation of lysine 27 in histone H3. Curr Opin Genet Dev 14: 155-164, 2004.
42. Kuzmichev A, Jenuwein T, Tempst P and Reinberg D: Different EZH2-containing complexes target methylation of histone H1 or nucleosomal histone H3. Mol Cell 14: 183-193, 2004.
43. Molloy PL and Watt F: DNA methylation and specific protein-DNA interactions. Philos Trans R Soc Lond B Biol Sci 326: 267-275, 1990.
44. Ross JP, Rand KN and Molloy PL: Hypomethylation of repeated DNA sequences in cancer. Epigenomics 2: 245-269, 2010.
45. Digel W and Lubbert M: DNA methylation disturbances as novel therapeutic target in lung cancer: preclinical and clinical results. Crit Rev Oncol Hematol 55: 1-11, 2005.
46. Lin RK, Hsu HS, Chang JW, Chen CY, Chen JT and Wang YC: Alteration of DNA methyltransferases contributes to 5'CpG methylation and poor prognosis in lung cancer. Lung Cancer 55: 205-213, 2007.